The Astrophysical Journal, 690:L122–L125, 2009 January 10 doi:10.1088/0004-637X/690/2/L122

THE DETECTION OF INFRARED SiS BANDS IN SPECTRA OF S STARS

J. Cami[1,2], G. C. Sloan[3], A. J. Markwick-Kemper[4], Albert A. Zijlstra[4], C. W. Bauschlicher Jr.[5], M. Matsuura[6,7], L. Decin[8,9], and S. Hony[10]

[1] Department of Physics & Astronomy, University of Western Ontario, London, ON N6A 3K7, Canada; jcami@uwo.ca
[2] SETI Institute, 515 N. Whisman Road, Mountain View, CA 94043, USA
[3] Cornell University, Astronomy Department, Ithaca, NY 14853-6801, USA
[4] Jodrell Bank Centre for Astrophysics, School of Physics & Astronomy, University of Manchester, Manchester, UK
[5] NASA Ames Research Center, Mail Stop 230-3, Moffett Field, CA 94035, USA
[6] National Astronomical Observatory of Japan, Osawa 2-21-1, Mitaka, Tokyo 181-8588, Japan
[7] Department of Physics and Astronomy, University College London, Gower Street, London WC1E 6BT, UK
[8] Katholieke Universiteit Leuven, Instituut voor Sterrenkunde, Celestijnenlaan 200 D, B-3001 Leuven (Heverlee), Belgium
[9] Universiteit van Amsterdam, Sterrenkundig Instituut "Anton Pannekoek," Kruislaan 403, 1098 SJ Amsterdam, The Netherlands
[10] Laboratoire AIM, CEA/DSM - CNRS - University Paris Diderot, DAPNIA/SAp, 91191 Gif-sur-Yvette, France
Received 2008 October 17; accepted 2008 November 19; published 2008 December 19

ABSTRACT

We present *Spitzer* spectra of S stars, which are cool evolved stars with a C/O ratio near unity, some of which have enhanced s-process abundances. We present the detection of a strong and unusual band in the mid-infrared, at 13 μm, within the *N*-band window. Using quantum-chemically calculated line lists, and model spectra, we identify this band as the fundamental rovibrational band of SiS. Detection of the overtone band at 6.7 μm confirms the identification. Fitting the line profile shows that the molecule is located in relatively cool layers, at $T \sim 1500$ K. We discuss these results in the context of chemical equilibrium models. The observed strength of these bands in the cool S stars makes them a promising observational diagnostic tool for studying the atmospheres of brown dwarfs and exoplanets.

Key words: infrared: stars – molecular data – stars: AGB and post-AGB – stars: atmospheres

1. INTRODUCTION

As stars ascend the asymptotic giant branch (AGB), they burn helium in a series of thermal pulses which result in the dredge-up of the resulting carbon-enriched material to the photosphere of the star (e.g., Iben & Renzini 1983). In the process oxygen-rich AGB stars become carbon stars. Third dredge-up can leave a star with an enhanced C/O abundance ratio and enhanced s-process abundances. Those stars are the S stars, with optical spectra dominated by absorption bands from unusual (s-process) oxides like ZrO, LaO, and YO (Merrill 1922; Fujita 1939, 1941a, 1941b; Keenan 1954; Ake 1979), and weaker TiO bands. The class ranges from mildly enhanced stars (MS-type) to full-blown S stars, to the SC-type stars, reflecting the C/O ratio, with C/O = 0.5 increasing to 0.95 for S stars, and around unity for the SC stars (Zijlstra et al. 2004) which form an intermediate group toward the carbon stars (Smith & Lambert 1990).

The formation of CO will exhaust all of the carbon, and since C/O $\sim$ 1, most of the oxygen as well (Bidelman 1950), allowing for the formation of molecules and dust grains with chemistries not usually seen in O-rich or C-rich AGB stars (Yamamura et al. 2000). To investigate the infrared properties of these molecules and dust grains, the *Spitzer Space Telescope* observed 90 Galactic S stars with the Infrared Spectrograph (IRS: Houck et al. 2004). The stars were selected from the Stephenson S star catalog, based on their *K*-band magnitudes, red colors, and variability. Of the 90 stars in the sample, about 50 do not exhibit a significant dust excess in the mid-infrared nor spectral features due to circumstellar dust, and we refer to these objects as naked stars. Of these 50 naked stars, 18 show a strong and broad absorption band at 13 μm, which we identify as arising from SiS. Section 2 describes the spectroscopy, both observations and reductions. In Section 3, we explain how we identify the broad 13 μm band as SiS, and in Section 4, we discuss the consequences.

2. OBSERVATIONS AND DATA REDUCTION

The IRS data were obtained as part of a program to study 90 S stars in the Galaxy in *Spitzer* Cycle 3 (Program ID 30737; P.I.: S. Hony). All observations were made in the staring mode, with the target in two positions in each aperture. Processing started with the flatfielded images provided by the Spitzer Science Center (SSC pipeline 15.3). We subtracted background images from the images, then corrected bad pixels using the *imclean* procedure. For Short–Low (SL) backgrounds, we used data obtained in the other SL aperture (i.e., SL order 1 for SL order 2, and vice versa). For Long–Low (LL), we used data in the same order, but the opposite nod (nod differences). We extracted spectra from the images using the *profile*, *ridge*, and *extract* modules available in the SPICE package.

Spectra were then co-added and calibrated, using as standards HR 6348 for SL and HR 6348, HD 166780, and HD 173511 for LL. We removed discontinuities between orders by multiplicatively normalizing them upward to match the order best centered in the slit. Finally, we removed extraneous data from the ends of each order.

Figure 1 plots the 18 S stars with a 13 μm band, in Rayleigh–Jeans units ($\lambda^2 F_\nu$). These units will plot a true Rayleigh–Jeans tail as a horizontal line. Several absorption bands are apparent: the red tail of the CO fundamental at 4.65 μm, the strong SiO fundamental band with a bandhead at 7.55 μm, a strong band with a bandhead at 13 μm which we identify below as the SiS fundamental, and a weak feature at 6.7 μm which we identify as the SiS overtone. In this Letter, we will focus on two sources in particular: CSS 100 which shows one of the strongest 13 μm bands in our sample, and CSS 267, which shows a somewhat different, double-humped shape.

Many objects exhibit a shoulder in the SiO feature around 9.5 μm, including CSS 100 and CSS 267. The wavelength of this feature is reminiscent of absorption due to interstellar dust (silicates), and raises concerns about the need to apply

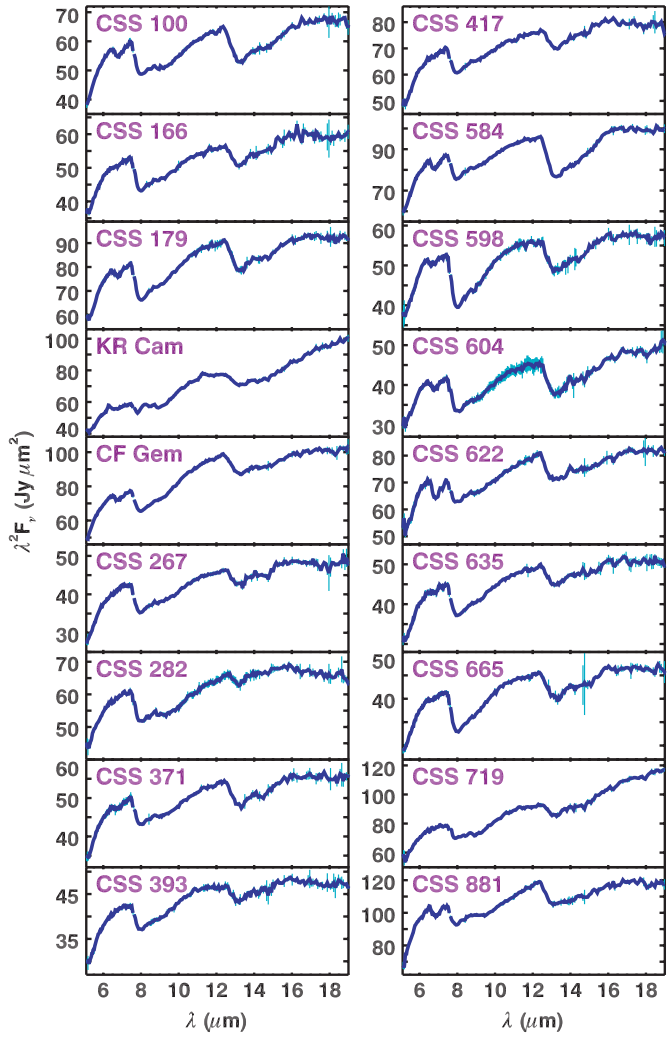

Figure 1. This figure shows the stars in our sample that clearly exhibit the SiS bands.

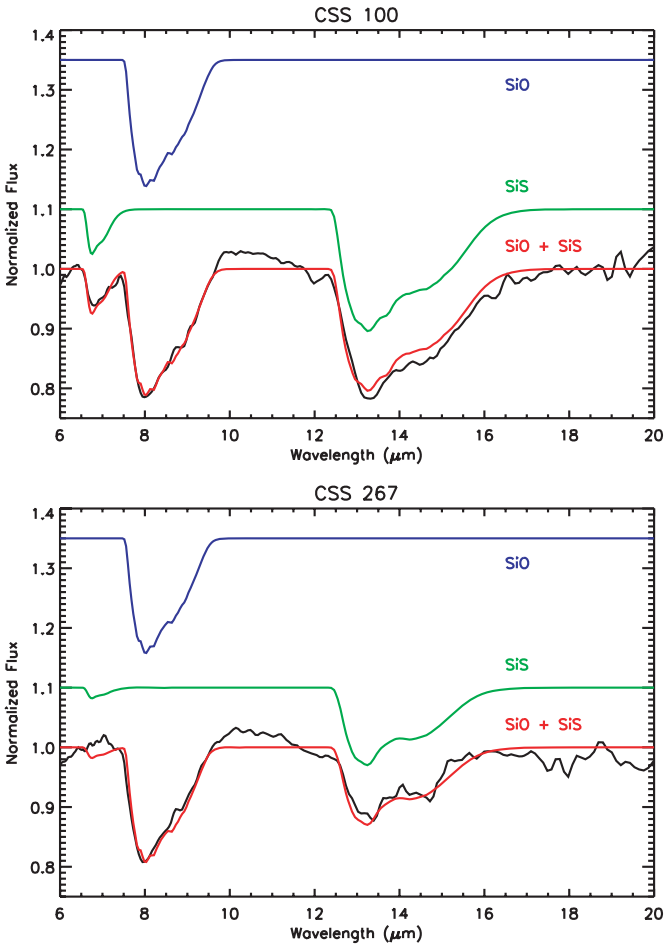

Figure 2. This figure shows the extinction-corrected spectra of CSS 100 (top) and CSS 267 (bottom) after division by a blackbody curve (black line; $T = 2900$ K for CSS 100 and T = 2700 K for CSS 267, respectively). The best fitting models for these two objects are overplotted (red), as are the individual contributions due to SiO (blue) and SiS (green). Note the clear presence of the SiS overtone band at 6.5 μm in the spectrum of CSS 100.

an extinction correction to our spectra. For the sources in our sample, no well-determined extinction values were found in the literature. We therefore used the extinction maps by Schlegel et al. (1998) to estimate $E(B-V)$ values and adopted standard conversion factors listed there to convert these to A_K values. From these maps, we find that $A_K = 0.4$ for CSS 100, and $A_K = 0.3$ for CSS 267. Such values are certainly high enough to leave a significant spectral footprint in the spectrum. We dereddened our spectra using the extinction curve by Chiar & Tielens (2006), using the local extinction curve, and adopting the A_K values quoted above. Figure 2 shows the resulting dereddened spectra. The extinction correction effectively removes the absorption shoulder at 9.5 μm and produces a band shape similar to our theoretical SiO profile.

3. THE SiS BANDS : IDENTIFICATION AND MODELING

Using molecular constants listed in Herzberg (1950), we tentatively identified the 13 μm band as an unresolved rovibrational band corresponding to the fundamental mode of SiS. To corroborate this identification, one of us (C.W.B.) calculated a state-of-the-art line list for rovibrational transitions due to SiS fundamental and overtone vibrational modes. Müller et al. (2007) presented a description of the energy levels in SiS as a series of Dunham coefficients which were obtained from careful analysis of laboratory measurements. Using the appropriate selection rules yields accurate frequencies for the individual transitions.

Calculating the intensities of the individual transitions requires knowledge of the dipole moment function. We performed an ab initio calculation for SiS with *Molpro 2006.1* (Werner et al. 2006) using the internally-contracted multireference configuration interaction (IC-MRCI) method (Knowles & Werner 1988a, 1988b), where the orbitals are optimized using the complete-active-space self-consistent-field (CASSCF) approach; we used the augmented-correlation-consistent polarized valence quintuple zeta (cc-pV5Z) sets developed by Woon & Dunning (1993). This yields a computed potential and dipole moment function.

The computed potential yields spectroscopic constants in good agreement with the experimental values in Müller et al. (2007); however, the computed bond length was found to be slightly larger than experimental values. We shifted the calculated dipole moment function by this difference. We next used the RKR1 program of Le Roy (2004) to generate a tabular potential from the experimental data by Müller et al. (2007). Finally, using the tabulated experimental potential and the shifted dipole moment the transition intensities (Einstein A

values) are computed for vibrational levels up to $v = 13$ and for rotational levels up to $J = 350$.[11]

With this line list, we then used the SpectraFactory engine (J. Cami et al. 2008, in preparation)[12] to calculate LTE single-slab model spectra for various temperatures and column densities. These model spectra are generated at the resolving power and oversampling rate corresponding to the *Spitzer* observations described in Section 2. To corroborate our identification, we tried to fit the 13 μm band in CSS 100 and CSS 267. The results are shown in Figure 2.

4. DISCUSSION

We find an excellent fit between the model spectra for SiS using the calculated line list and the observed profile of the 13 μm band. Additionally, in the spectrum of CSS 100, the overtone band at 6.7 μm (Aoki et al. 1998) appears at the proper absorption depth in our model, corroborating that the 13 μm band is indeed due to SiS. Individual SiS lines at 13.5 μm have previously been detected in the carbon star IRC+10 216 (Boyle et al. 1994), where the lines are heavily blended with C_2H_2. Detection of the broad band is possible because of the absence of C_2H_2 and HCN in the (oxygen-rich) S stars.

While the absorption depth of the SiO band in both sources is roughly the same, the absorption depth of the SiS band at 13 μm differs by about a factor of 2. Moreover, the SiS band is clearly broader in CSS 100 than it is in CSS 267, and in the latter spectrum, the SiS overtone is hardly visible. This difference is reflected in the parameters corresponding to the best fit. The fit parameters for SiO are: $T = 800$ K and $N = 7.9 \times 10^{21}$ cm^{-2} for CSS 100, and $T = 800$ K and $N = 3.2 \times 10^{21}$ cm^{-2} for CSS 267—reflecting primarily a very high optical depth in both objects. For the SiS bands, on the other hand, we find $T = 1500$ K and $N = 5.0 \times 10^{19}$ cm^{-2} for CSS 100, and $T = 1600$ K and $N = 1.0 \times 10^{19}$ cm^{-2} for CSS 267. So, while the SiO band in both cases is very optically thick and therefore yields very similar parameters, the column densities for SiS differ by about a factor of 5. The other objects shown in Figure 1 do exhibit much more obvious variations in the profiles of the SiO bands, and there is no clear relation between the absorption depth or width of the SiO band and that of the SiS bands. This implies that the column densities of SiO and SiS in S stars vary independently of each other.

The strength of the overtone band roughly scales with the fundamental in Figure 1, but there are some exceptions, e.g., CSS 166. This may be related to the temperature structure of the extended envelope.

Figure 3 shows the results of chemical equilibrium calculations (Markwick 2000). These use solar abundance ratios with a varying carbon abundance to obtain a range of C/O ratios. The SiO partial pressure is sensitive mainly to the C/O ratio, dropping off sharply when C/O > 0.95, but has little dependence on temperature. SiO is among the most stable molecules in stellar atmospheres and is abundant as long as sufficient free oxygen is available. SiS has a reverse dependence on C/O ratio, but it benefits from a lower temperature. Therefore, the SiS/SiO ratio will increase when C/O > 0.9, and/or $T < 2200$ K. The enhancement of the SiS abundance relative to the SiO abundance is as much as two orders of magnitude as the C/O ratio grows above 0.9. We do not see such an extreme change here, but the

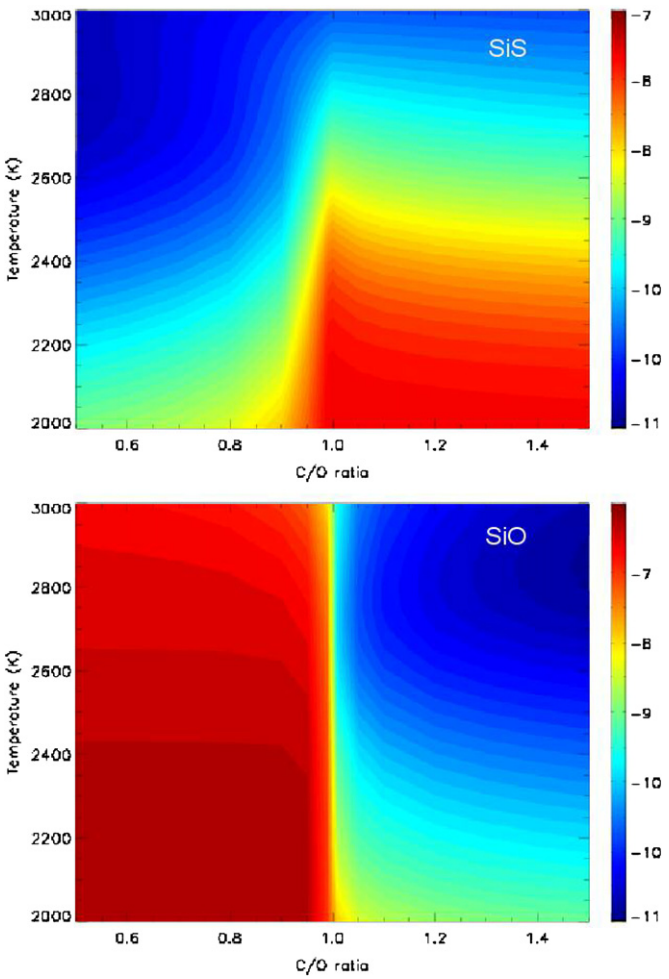

Figure 3. The equilibrium partial pressures of SiS (top) and SiO (bottom) as a function of temperature and C/O ratio.

S stars do show a large enhancement compared to normal M-type AGB stars where SiS is not detected.

The sulfur chemistry in stellar envelopes depends dramatically on the C/O ratio. In carbon stars, much of the sulfur is in CS, driving an extensive chemistry toward organo-sulfur chains (Millar et al. 2001). In oxygen-rich environments, S is locked into SO and SO_2, both of which have only weak infrared features (Yamamura et al. 2000). The fact that only 1/3 of the naked S stars in our sample show the SiS band is probably related to the sensitivity to C/O ratio. Metallicity may also play a role. At higher metallicity, more carbon dredge-up is required to obtain the same C/O ratio. This is clearly seen in Magellanic Cloud carbon stars, where the acetylene bands become much stronger at low metallicity, indicating higher C/O ratios (Matsuura et al. 2005; Zijlstra et al. 2006; Sloan et al. 2006). These stars will also show a lower Si abundance, but the sensitivity of the SiS abundance to C/O ratio is much more dramatic.

Yamamura et al. (2000) discuss the equilibrium sulfur chemistry in S star envelopes. They argue that SH is the first sulfur molecule to form in the hot layers. At temperatures below 1500 K H_2S and SiS replace it. Yamamura et al. (2000) detect infrared SH bands in the S star R And, and show it is found only in a thin layer at $T \sim 2200$ K. We find a temperature of 1500 K for the SiS, entirely consistent with their prediction.

[11] An electronic version of the line list is available from Vizier.
[12] http://www.spectrafactory.net

The chemical equilibrium models (Figure 3) predict a stratification where the SiS is dominant in the upper extended atmosphere and the SiO dominates in the hotter stellar photosphere. We do not see this, however: the SiO temperature in our fit is well below that of the SiS, and neither is photospheric. The SiS temperature is reasonable, as mentioned above, but the low SiO temperature is more surprising. The SiO absorption will be dominated by molecules outside the continuum-emission layer at 8 μm. The continuum in S stars is due to H^- absorption. Water vapor (Markwick & Millar 2000) could contribute at 8 μm but the near-infrared bands have not been detected in ISO/SWS spectra of S stars.

Sub-mm lines from SiS are detected in the outer envelopes of carbon stars (e.g. Bieging & Tafalla 1993), and at much lower abundances, also in M-type AGB stars (Schöier et al. 2007). Decin et al. (2008) have reported higher J transitions in some S stars. The final abundance in the M-type stars may depend on the temperature at which the chemistry freezes out. However, there is evidence for nonequilibrium sulfur chemistry, possibly caused by pulsation shocks, which modifies abundances of SiS and SO_2 (Yamamura et al. 2000; Decin et al. 2008). Bieging & Tafalla (1993) argue that, in carbon stars, the sub-mm lines indicate that SiS disappears in the dust formation region, most likely because Si is adsorbed into the dust and the released sulfur forms CS. However, Schöier et al. (2007) found no strong evidence that SiS depletes in the outflow. Proposed condensates in S stars are FeSi (Ferrarotti et al. 2000) and troilite (FeS: Hony et al. 2002). The role of SiS in oxygen-rich dust formation is not known.

The fact that such a major broad band at 13 μm, with the band head located within the N-band window, had not previously been detected shows that our understanding of the molecular bands in the mid-infrared is still limited. We do not find evidence of strong additional bands. As Figure 2 shows, SiS fits the 13 μm bands well; the only potential issue is a possible absorption wing at 12 μm. However, weaker additional absorption bands would not be unexpected. For instance, the molecules which dominate the optical (TiO, ZrO, VO, YO) do not have known mid-infrared counterparts.

The finding in this Letter could be of importance for the study of atmospheres of brown dwarfs. Brown dwarfs exhibit molecular atmospheres (see, e.g., Mainzer et al. 2007; Morrow et al. 2008), where abundances of trace species are typically used as important diagnostic tools for understanding nonequilibrium chemistry and physical aspects (e.g., temperature structure) in such objects. Indeed, SiS is considered a tracer of weather in substellar objects (Visscher et al. 2006). Its presence in brown dwarfs could, as in the S stars presented here, be detected as a 13 μm band in the N-band.

These observations were obtained with the *Spitzer Space Telescope*, operated by JPL, California Institute of Technology under NASA contract 1407.

Facilities: Spitzer

REFERENCES

Ake, T. B. 1979, ApJ, 234, 538
Aoki, W., Tsuji, T., & Ohnaka, K. 1998, A&A, 340, 222
Bidelman, W. P. 1950, ApJ, 112, 219
Bieging, J. H., & Tafalla, M. 1993, AJ, 105, 576
Boyle, R. J., Keady, J. J., Jennings, D. E., Hirsch, K. L., & Wiedemann, G. R. 1994, ApJ, 420, 863
Chiar, J. E., & Tielens, A. G. G. M. 2006, ApJ, 637, 774
Decin, L., Cherchneff, I., Hony, S., Dehaes, S., De Breuck, C., & Menten, K. M. 2008, A&A, 480, 431
Ferrarotti, A., Gail, H.-P., Degiorgi, L., & Ott, H. R. 2000, A&A, 357, L13
Fujita, Y. 1939, Japan. J. Astron. Geophys., 17, 17
Fujita, Y. 1941a, Japan. J. Astron. Geophys., 18, 45
Fujita, Y. 1941b, Japan. J. Astron. Geophys., 18, 177
Herzberg, G. 1950, Molecular Spectra and Molecular Structure 1, Spectra of Diatomic Molecules (2nd ed.; New York: Van Nostrand Reinhold)
Hony, S., Bouwman, J., Keller, L. P., & Waters, L. B. F. M. 2002, A&A, 393, L103
Houck, J. R., et al. 2004, ApJS, 154, 18
Iben, I., & A., Jr., Renzini 1983, ARA&A, 21, 271
Keenan, P. C. 1954, ApJ, 120, 484
Knowles, P. J., & Werner, H. J. 1988a, Chem. Phys. Lett., 145, 514
Knowles, P. J., & Werner, H. J. 1988b, J. Chem. Phys., 89, 5803
Le Roy, R. J. 2004, RKR1 2.0: A Computer Program Implementing the First-Order RKR Method for Determining Diatom Potential Energy Curves, Univ. of Waterloo, Chem. Phys. Res. Rep., CP-657R, 2004
Markwick, A. 2000, PhD thesis, UMIST
Markwick, A. J., & Millar, T. J. 2000, A&A, 359, 1162
Mainzer, A. K., et al. 2007, ApJ, 662, 1245
Matsuura, M., et al. 2005, A&A, 434, 691
Merrill, P. W. 1922, ApJ, 56, 45
Millar, T. J., Flores, J. R., & Markwick, A. J. 2001, MNRAS, 327, 1173
Morrow, A. L., et al. 2008, ApJ, 676, L143
Müller, H. S. P., et al. 2007, Phys. Chem. Chem. Phys., 9, 1579
Schlegel, D. J., Finkbeiner, D. P., & Davis, M. 1998, ApJ, 500, 525
Schöier, F. L., Bast, J., Olofsson, H., & Lindqvist, M. 2007, A&A, 473, 871
Sloan, G. C., Kraemer, K. E., Matsuura, M., Wood, P. R., Price, S. D., & Egan, M. P. 2006, ApJ, 645, 1118
Smith, V. V., & Lambert, D. L. 1990, ApJS, 72, 387
Visscher, C., Lodders, K., & Fegley, B. J. 2006, ApJ, 648, 1181
Werner, M. W., et al. 2004, ApJS, 154, 1
Werner, H. J., et al. 2006, MOLPRO, version 2006.1 (a package of ab initio programs; see http://www.molpro.net)
Woon, D. E., & Dunning, T. H. 1993, J. Chem. Phys., 98, 1358
Yamamura, I., Kawaguchi, K., & Ridgway, S. T. 2000, ApJ, 528, L33
Zijlstra, A. A., et al. 2004, MNRAS, 352, 325
Zijlstra, A. A., et al. 2006, MNRAS, 370, 1961